International Journal of Advanced Chemistry, 14(2) (2026) 16-27

International Journal of Advanced Chemistry

Website: www.sciencepubco.com/index.php/IJAC
https://doi.org/10.14419/ay2sec19
Research paper

Rate Kinetics of Hydrazine Decomposition Using Pt/Sio2 Catalyst in A Nitric Acid Medium for Nuclear Fuel Reprocessing

S.Ganesh *, Sanat Karmakar, Rahul Trika

Reprocessing Design and R&D Group, Reprocessing Group, Indira Gandhi Centre for Atomic Research, Kalpakkam - 603102, Tamil Nadu, India
**Corresponding author E-mail: gans@igcar.gov.in*

Received: 9 Jul 2026, Accepted: 19 Oct 2026, Published: 23 Nov 2026

Abstract

Catalytic decomposition of hydrazine nitrate is essential for the disposal of hazardous chemicals. In the present study, the kinetics of hydrazine decomposition (0.5 M) over a Pt/SiO2 heterogeneous catalyst in a nitric acid medium (1 - 3 M HNO3) have been systematically investigated. Batch experiments were conducted under varying conditions of temperature (313 - 343 K), catalyst amount (0 - 10 g), and mixing speed (100 - 500 rpm) to elucidate the reaction and optimize it. The apparent rate constant was determined from the experimental conditions and compared across different catalyst particle sizes. The activation energy for this reaction is 47.88 kJ/mol, determined from experimental data-fitting analysis using a pseudo-first-order reaction order. Increased catalyst loading enhanced the reaction rate, confirming the surface-mediated catalytic pathway. The rate constant increased with temperature, indicating a chemical-controlled regime. The influence of nitric acid concentration revealed a dual role: acting both as a reactant and an inhibitor at higher concentrations due to surface-site competition. The study provides valuable kinetic parameters and improves process safety by enabling controlled removal of excess hydrazine in nitric acid streams in nuclear reprocessing.

Keywords: *Hydrazine Nitrate; Decomposition; Pt/SiO_2 Catalyst; PUREX Process; Kinetics; Pseudo-First-Order.*

1. Introduction

Spent nuclear fuel reprocessing is an essential step in the closed nuclear cycle, enabling the recovery of valuable fissile materials such as uranium and plutonium. Among the various reprocessing technologies, the PUREX (Plutonium–Uranium Redox EXtraction) process remains the most widely used for separating uranium and plutonium from irradiated fuel, using tri-n-butyl phosphate in a nitric acid medium [1-3]. Hydrazine (salt-free reagent) acts as an effective scavenger for nitrous acid formed through radiolysis of nitric acid and stabilizes plutonium oxidation states in nitric acid solutions [4-5]. It also serves as an anticorrosive protective agent in the primary and secondary circuits of nuclear power plants [6]. However, during reprocessing, uncontrolled accumulation of hydrazine in nitric acid streams can cause operational and safety issues [7]. Currently, a commonly employed method for their removal is to introduce an oxidant (such as sodium nitrite or nitrogen dioxide) [8], which generates a large amount of alpha waste and creates disposal issues. The efficient removal or destruction of these species from nitric acid waste streams is an important step in minimizing secondary waste and ensuring process safety. In the literature, the thermal decomposition of hydrazine nitrate in nitric acid involves a complex multi-step reaction (leading to an exothermic process) and the formation of nitrogen oxides (in situ generation of gaseous products such as N_2 and nitrous oxides), which can complicate waste treatment operations [9-10]. A heterogeneous noble-metal catalyst with promising activity toward the decomposition of hydrazine nitrate in a nitric acid medium offers a safe, environmentally friendly approach. Despite these advantages, hydrazine is thermodynamically unstable in strongly oxidizing nitric acid environments and can decompose rapidly in the presence of catalytic species.

In nuclear fuel reprocessing streams, noble metals such as Ru, Rh, Pd, and Pt are present either as fission products or as structural (Fe(III), Cr(III), Cu(II), Ni(II)) and catalytic materials. These metals exhibit vigorous catalytic activity in the decomposition of hydrazine. These species act as homogeneous catalysts, significantly enhancing the rate of hydrazine decomposition even at trace concentrations. These metals are known to catalyze redox reactions involving hydrazine and nitrogen oxides. In particular, platinum-based materials exhibit high activity for hydrazine decomposition because platinum facilitates N-N bond cleavage and promotes dehydrogenation even in strongly acidic environments. Hydrazine adsorption on Pt sites leads to stepwise dehydrogenation and formation of surface-bound intermediates such as NH_2* and N_2H_x*. In nitric acid media, nitrate and nitrous acid act as oxidants, regenerating active Pt sites and producing gaseous nitrogen and nitrogen oxides. The catalytic performance depends strongly on parameters such as catalyst loading, temperature, nitric acid concentration, and hydrodynamic conditions.

Copyright ©S. Ganesh et al. This is an open access article distributed under the Creative Commons Attribution License, which permits unrestricted use, distribution, and reproduction in any medium, provided the original work is properly cited.

Platinum-supported catalysts, such as Pt/SiO_2, have attracted interest due to their high catalytic activity, chemical stability in acidic media, and corrosion resistance. It is the most promising system for understanding noble-metal–catalyzed hydrazine decomposition in nitric acid media. One significant advantage of using platinum as a catalyst is that it prevents the formation of hydrazoic acid (HN_3). This is because the HN_3 adsorbed on the catalyst surface is not desorbed into solution but instead undergoes catalytic decomposition on the platinum surface [11]. Recent studies have shown that supported metal catalysts (e.g., Pt/SiO_2, Ru/C, and Ru/ZSM-5) can efficiently decompose hydrazine nitrate in nitric acid solutions relevant to nuclear waste streams [12-25]. A large quantity of work on the decomposition of hydrazine in the presence of various catalytic materials has been reported [26]. The kinetics of the catalytic decomposition of hydrazine in nitric acid were studied by Li et al. and Zhang et al. [13, 18]. Despite extensive studies on hydrazine decomposition in neutral and alkaline systems, limited information is available for Pt-catalyzed decomposition under highly acidic PUREX-relevant conditions. Therefore, a laboratory-scale study was conducted to optimize reaction parameters for implementation in the reprocessing plant. The influence of temperatures between 313K and 343K, the amount of catalyst, the effect of nitric acid, and the impeller mixing speed (RPM) on homogeneous mixing were studied in batch mode.

2. Experimental

2.1. Materials and methods

All chemicals were of analytical grade and 99.90% pure (Sigma-Aldrich and Merck) and were used. All solutions were prepared using deionized water. A standard hydrazine hydrate solution (about 18.5 M) was procured from Orion Chem. Pvt. Ltd., Mumbai. Para-(dimethylamino) benzaldehyde (pDMAB) with 98.90% purity was obtained from BDH Prolabo, Chennai, and used for the spectrophotometric analysis of hydrazine. A fine powder of Pt/SiO_2 catalyst was procured from Hindustan Platinum Limited, Mumbai, with a specific Pt loading of 2%. The catalytic performance was already studied in the same laboratory and reported [27]. UV-Vis spectrophotometer supplied by Thermo Scientific India Pvt. Limited use for absorbance measurements. A digital pH meter, model Micro-07, supplied by Chemlabs, was used to adjust pH. Tapson's analytical single pan balance model 200 T with 0.001 g accuracy for weighing. The temperature controller MIC-66A (±0.10ºC) was obtained from Modern Scientific Instrument Company, Mumbai. Acid-base titration was carried out using a PC based automatic titration system from Metrohm. Sieving was done using a Vibrator Sieve Shaker, RETSCH make, Model AS200, with sieves of different particle sizes, like 63, 38, and 20 microns, to separate the fine powder.

2.2. Analytical methods

A 2 L stock solution of 0.5 M hydrazine nitrate was prepared by dissolving 54.05 mL of hydrazine hydrate (18.5 M) in 1.5 M nitric acid. The same procedure was followed to prepare 500 mL stock solutions of 2.5 M and 3 M nitric acid. The working solution was standardized by the sequential titrimetry method using a standard Na_2CO_3 solution [28-29]. In contrast, lower concentrations of hydrazine were analysed by spectrophotometry using the p-dimethylaminobenzaldehyde (pDMAB) chromogenic reagent [30]. In an acidic medium, hydrazine nitrate undergoes a condensation reaction with pDMAB to form a yellow hydrazone. The absorbance of the resulting solution is measured at 457 nm. Within a certain range, the concentration of hydrazine is directly proportional to the measured absorbance. A standard curve was obtained by plotting the mean absorbance for each standard concentration against the target hydrazone concentration. Typical absorption spectra and calibration curves for hydrazine-pDMAB are shown in Fig.1 and Fig.2, respectively. They indicate a good linear relationship between absorbance and concentration from 4.0 × 10^-7 to 6.4 x 10^{-5}M. A comparative study of the proximity to the real value and the variation between the two methods is reported in Table 1.

Table 1: Comparison of the Hydrazine Concentration by Titrimetry and Spectrophotometry

	Titrimetry		Spectrophotometry [30]	
	$[N_2H_4]$, M	RSD (%)	$[N_2H_4]$, M	RSD (%)
Std 1	0.5255±0.014	0.68	0.527±0.034	2.42
Std 2	0.246±0.023	0.79	0.246±0.023	1.41
Std 3	0.184±0.063	1.48	0.184±0.069	0.89
Std 4	0.107±0.084	2.04	0.109±0.034	0.77
Std 5	0.382±0.014	0.93	0.382±0.014	1.58
Std 6	0.411±0.094	2.34	0.0517 ± 0.021	0.76
Std 7	0.052±0.214	1.26	0.0518 ± 0.0062	0.23

2.3. Batch experiments

The kinetic experiments were performed in a double-jacket glass reactor equipped with a temperature controller (Julabo HE circulator) and a vertical stirrer impeller (rotor) to maintain constant interaction between the solid solute and the liquid phase, as shown in Fig. 3. Batch experiments were conducted in a temperature-controlled reactor with continuous stirring. A given volume (100 mL) of working solution containing a calculated amount of nitric acid and hydrazine (0.5 M hydrazine nitrate in 1 M nitric acid) is put into the reactor. A weighed portion of catalyst, preliminarily heated to the experimental temperature, is then added.

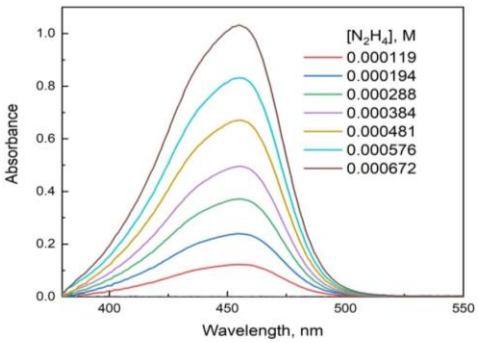

Fig. 1: Typical Absorption Spectrum of Hydrazine Using pDMAB.

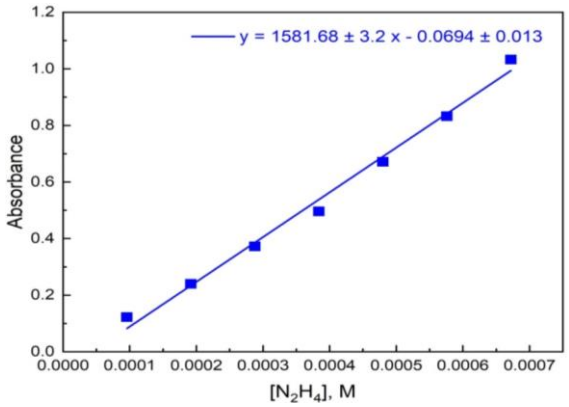

Fig.2: Typical Calibration Curve of Hydrazine Using pDMAB.

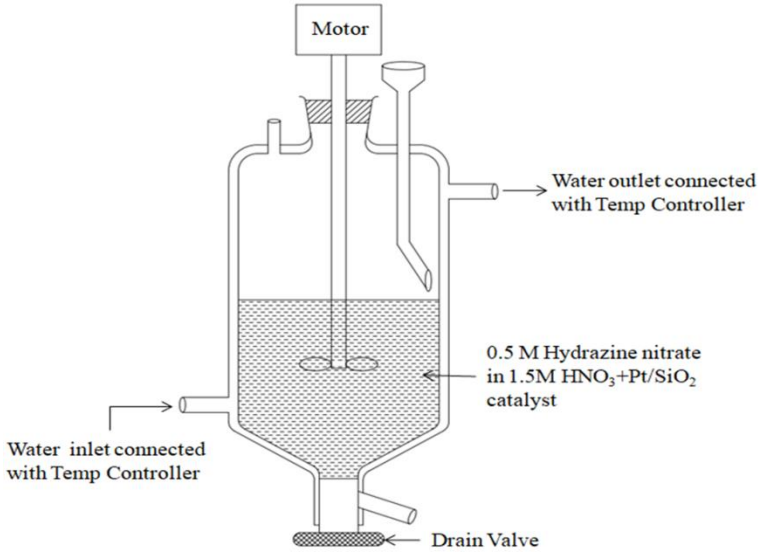

Fig. 3: Temperature-Controlled Mixing Reactor with Mechanical Agitator.

A glass shaft with an impeller attached and an RPM controller was then immersed in the solution to achieve a controlled mixing rate. The concentrations of mineral acid and hydrazine were periodically measured by the sequential (acid-base) titrimetric method with a standard Na_2CO_3 solution and by the spectrophotometric method [30]. Similarly, batch experiments were conducted to optimize parameters, including temperature, catalyst amount, mixing rate (RPM), and nitric acid concentration, for hydrazine decomposition as shown in Table 2. Reaction rates were determined by monitoring the decrease in hydrazine concentration with time. The effects of temperature and catalyst concentration were studied to evaluate reaction order and activation energy. During all batch experiments to measure hydrazine concentration, 0.5 mL of the supernatant from the Pt/SiO_2-hydrazine nitrate mixture was collected at different time intervals. The fine particles of the catalyst were removed by centrifugation, and hydrazine was estimated after color development with the chromogenic agent (pDMAB), with suitable dilution if required. Typical UV-Vis absorption spectra for the decomposition of hydrazine nitrate over the Pt/SiO_2 catalyst are shown in Fig. 4.

Table 2: Experimental Conditions to Optimize Various Parameters on Decomposition of Hydrazine.

Parameter	Temp (K)	Catalyst (g)	Mixing (rpm)	HNO_3(M)
Effect of temperature	313	8	500	1.5
	323			
	333			
	343			
Effect of the amount of catalyst	333	0	500	1.5
		4		
		6		

		8 10		
Effect of mixing speed	333	8	200 300 400 500	1.5
Effect of acidity	333	8	500	1.5 2.0 2.5

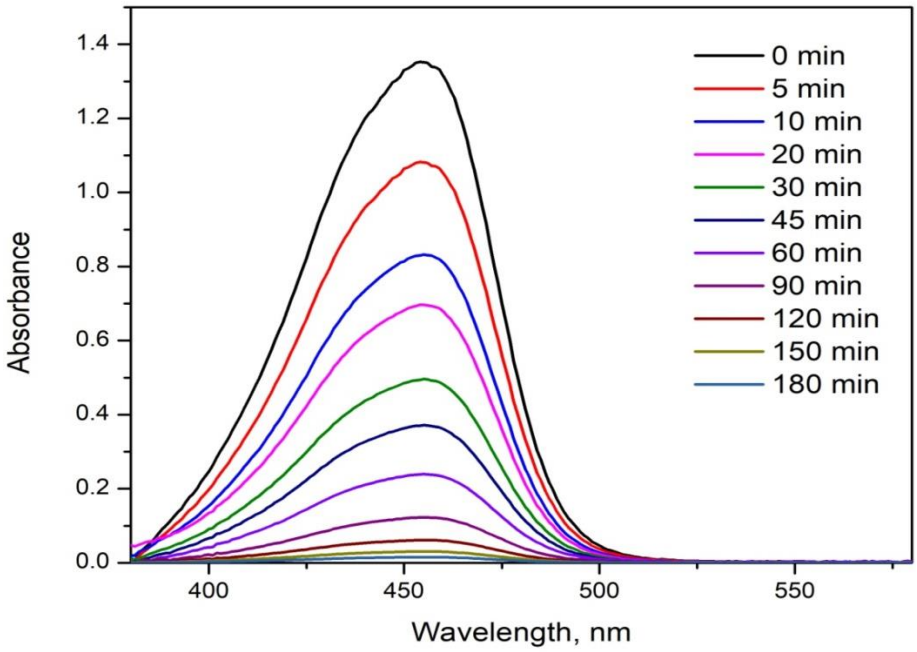

Fig. 4: Typical UV-Vis Absorption Spectrum for the Process of the Decomposition of Hydrazine Nitrate Over the Pt/Sio_2 Catalyst with Time.

3. Results and Discussion

The catalytic decomposition of hydrazine in a nitric acid medium was studied in the presence of a solid catalyst, 1% Pt/SiO_2, and kinetic experiments were performed in a batch reactor under the optimized conditions listed in Table 2. The heterogeneous catalytic decomposition of hydrazine in nitric acid medium in the presence of Pt/SiO_2 catalyst [11] occurs with the formation of NH_4^+ ions and of N_2O and N_2:

$$36N_2H_5NO_3 + 2HNO_3 \rightarrow 20NH_4NO_3 + 32N_2 + 3N_2O + 51\,H_2O$$

The kinetic studies for the decomposition of hydrazine nitrate were carried out at 313-333 K with 8 g of 1% Pt/SiO_2 catalyst. The initial concentrations of hydrazine nitrate and nitric acid were 0.5 M and 1 M, respectively. The hydrazine nitrate concentration as a function of reaction time at different temperatures was plotted and fitted to a first-order equation.$d[N_2H_5NO_3]/dt = -k[N_2H_5NO_3]^1$.

The variation in hydrazine concentration over time at different temperatures, nitric acid concentrations, catalyst amounts, and mixing speeds was analyzed to determine the reaction kinetics. Assuming a first-order dependence of the oxidation rate on hydrazine concentration, the data were fitted according to the integrated rate expression as given by $\ln(C/C_o) = -kt$, where C and C_o are the hydrazine concentrations at a particular time t and its initial concentration at t=0, respectively, and k is the apparent first-order rate constant. The linearity of $\ln(C/C_o)$ vs. time plots indicated good correlation (R^2) ranging from 0.99 to 0.88, confirming that hydrazine decomposition under the applied conditions follows pseudo-first-order kinetics. The evaluated rate constants, along with the parameters such as temperature, catalyst amount, mixing speed, and nitric acid concentration, are summarized in Table 3. These results indicate that comparing reaction rates for the catalytic decomposition of hydrazine shows that the pseudo-first-order reaction model can well describe the reaction kinetics as a function of temperature, mixing speed, and catalyst amount, but is not suited to nitric acid concentration.

Table 3: Influence of Experimental Conditions on the Apparent First-Order Rate Constants (K) of Decomposition of Hydrazine in Nitric Acid on Pt/Sio_2 Catalyst

Parameter	Rate constant (k)/ min^{-1}	R^2 value
Temperature (K)		
313	0.1193	0.972
323	0.1764	0.921
333	0.2575	0.948
343	0.5147	0.878
Catalyst amount (g)		
0	0.0165	0.957
4	0.0329	0.964
6	0.0439	0.979
8	0.0735	0.982
10	0.0978	0.997
Mixing speed (RPM)		
200	0.066	0.695

300	0.117	0.798
400	0.147	0.819
500	0.238	0.997
Acidity (M)		
1.5	0.075	0.912
2.0	0.095	0.733
2.5	0.109	0.703

3.1. Effect of mixing rate

The influence of mixing rate on the catalytic decomposition of hydrazine in a nitric acid medium was studied to assess the presence of external (liquid-solid) mass-transfer limitations. It concerns the diffusion of the reactants through the interface between the liquid and the solid. This is influenced by three main factors: the catalyst surface, the catalyst thickness, and the concentrations of both hydrazine and nitric acid. External mass transfer involves the diffusion of reactant species across the stagnant hydrodynamic boundary layer surrounding the solid catalyst particles. The rate of this transport is primarily governed by hydrodynamic conditions (agitation intensity), the physical properties of the fluid, and particle external surface area. The surface area and dimension (thickness) of the catalyst are strictly linked to the amount of catalyst used, which is kept constant for a given catalyst amount. Experiments were carried out in the presence of the solid catalyst Pt/SiO_2 under the following conditions: $[N_2H_5^+]$ = 0.5 M; $[H^+]$ = 1.5 M; T = 333 K, and agitation speeds ranging from 200 to 500 RPM (with a fixed catalyst loading). Experiments consisted of mixing, i.e., the interaction between two phases: a solid catalyst and a hydrazine solution. The linear plots of ln(C/Co) vs. time were obtained at different mixing speeds, confirming the applicability of pseudo-first-order kinetics under the experimental conditions, as shown in Fig. 5. The apparent first-order rate constants (k) were calculated from the slopes of these plots. As the mixing speed increased from 200 to 500 RPM, the apparent rate constant increased substantially from 0.066 min^{-1} to 0.238 min^{-1}, while the correlation coefficient (R^2) improved from 0.695 to 0.997, as indicated in Table 3. The higher RPM solute-solid (catalyst) interaction is due to the solute penetrating the solvent film more easily before reaction with the catalyst.

Reaction products are more readily removed from the catalyst surface (which may improve the mass transport of hydrazine to the surface). As a result, the apparent rate constants (k) become independent of mixing intensity. This indicates the elimination of external diffusion limitation and confirms that the reaction is under kinetic control. At lower stirring rates, diffusion of hydrazine from the bulk solution to the catalyst surface may limit the overall reaction rate. At low stirring speeds (200 and 300 rpm), the same amount of hydrazine took longer to decompose, indicating both intrinsic surface reaction kinetics and external mass-transfer resistance. Insufficient mixing leads to the formation of a diffusion boundary layer around catalyst particles, restricting the transport of hydrazine molecules to active Pt sites. For these reasons, deviations from an ideal first-order kinetic model result in lower R^2 values. As the stirring speed increases to 500 RPM, the rate constant and the correlation coefficient increase, suggesting that external diffusion limitations are minimized, and the system approaches intrinsic kinetic control, thereby enhancing the fluid-particle relative velocity and expediting reactant transport to the active surface sites. Further, increasing the mixing speed yields no significant increase in the apparent rate constant. It compromises the stability of the rotation axis, potentially leading to solution droplets on the reactor walls. The reaction exhibits apparent first-order behaviour predominantly under optimized hydrodynamic conditions (500 rpm), where external mass-transfer limitations are minimized, preventing vortex formation and shaft vibration. So, 500 rpm was chosen as the optimal mixing speed for these studies. Comparison studies of apparent rate constants across different particle sizes were conducted, and the results are summarized in Table 4.

Table 4: Influence of Mixing Speed in Comparison on the Apparent First-Order Rate Constants (K) of Decomposition of Hydrazine in Nitric Acid on Pt/Sio_2 Catalyst

	Rate constant, min^{-1}		
RPM	68 micron	38 micron	20 micron
200	0.035	0.052	0.066
300	0.047	0.079	0.117
400	0.102	0.128	0.147
500	0.135	0.189	0.238

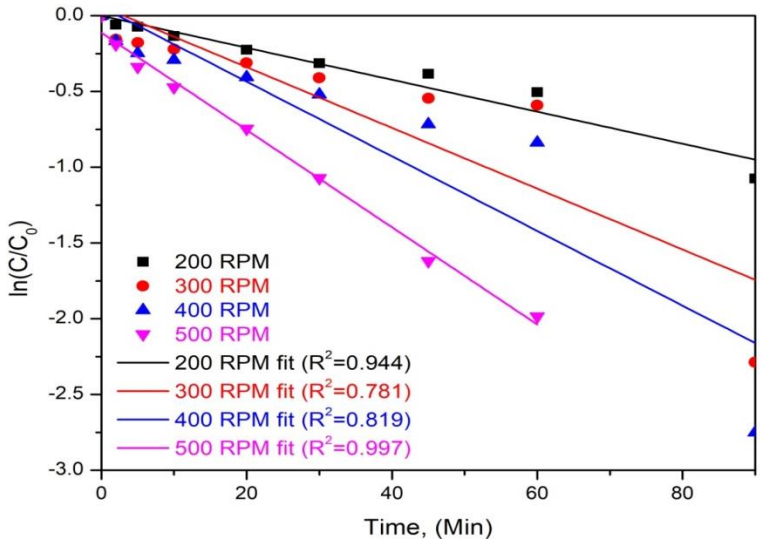

Fig. 5: Influence of Mixing Speed on the First-Order Kinetic Plots for the Decomposition of Hydrazine Over Pt/Sio_2. $[N_2H_4]$ = 0.5 M, $[HNO_3]$ = 1.5 M, Catalyst Amount = 8 G, Temp = 333 K, Varying the Mixing Speed From 200 To 500 RPM

Across all tested particle sizes (20 µm, 38 µm, and 68 µm), the apparent rate constant increased with agitation speed, indicating boundary-layer thinning across all fractions and at any given mixing speed. Smaller catalyst particles yielded systematically higher rate constants (e.g., at 500 RPM, k = 0.238 min^{-1} for 20 µm versus 0.135 min^{-1} for 68 µm). It clearly indicated that the smaller-particle-size catalyst has an apparent rate constant that is highly sensitive to mixing speed and strongly influenced by external mass-transfer resistance, compared with the larger-particle-size catalyst.

3.2. Effect of amount of catalyst

The influence of catalyst amount on the rate of catalytic decomposition of hydrazine in a nitric acid medium was examined by varying the amount of Pt/SiO_2 catalyst while keeping other parameters constant. These catalytic tests were performed by varying the catalyst amount from 0 to 10 g. This range was chosen for the minimum amount of catalyst required, which would have required sufficient time to complete the reaction and generate good data. The $\ln(C/C_o)$ versus time plots remained linear for all catalyst loadings, indicating that the pseudo-first-order assumption is valid across the studied range. The apparent rate constants (k) were determined from the slopes of the plots shown in Fig.6, which showed good correlation (R^2 = 0.957 to 0.982). It was observed that the kinetics followed pseudo-first-order behavior with respect to hydrazine concentration, as confirmed. From this, hydrazine decomposition took a longer time in the absence of a catalyst, highlighting the importance of a catalyst. With 4 and 6 g of catalyst, decomposition of hydrazine is less effective, i.e., the reaction is slower than with 8 g. Experiments were also carried out with 10 g of catalyst, showing a much greater difference in decomposition compared to 8 g. It is also confirmed that the apparent rate constants (k) increase with increasing catalyst amount, indicating that the effective active area increases, as summarized in Table 3. Sample collection with 10 g was difficult because the sample contained a higher catalyst content, which interfered with the analysis. Moreover, the high cost of noble metal catalysts reduces the economic feasibility of a large-scale system, and catalyst replacement or regeneration is straightforward. Hence, the amount of catalyst under the desired conditions was optimized to 8 g.

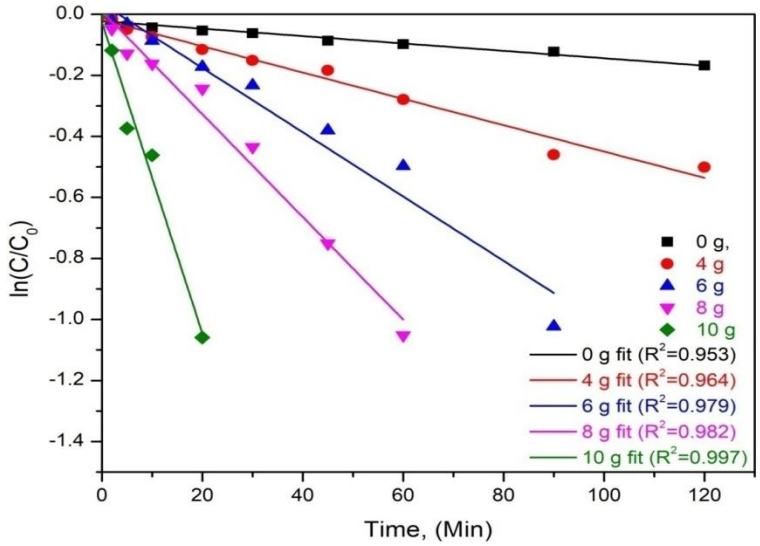

Fig. 6: Influence of Catalyst Amount on the First-Order Kinetic Plots for the Decomposition of Hydrazine Over Pt/Sio_2. $[N_2H_4]$ = 0.5 M, $[HNO_3]$ = 1.5 M, RPM = 500, Temp = 333 K, Varying Catalyst Amount From 0 To 10 G

The effect of the Pt/SiO_2 catalyst particle size was studied by using catalysts with different average particle diameters while maintaining a constant catalyst amount. From Table 5, a clear dependence of reaction rate on particle size was observed, and an inverse relationship with the apparent rate constant. The smaller particle size, particularly 20 µm particles, was not adopted for the following reasons: (i) due to very fine particles, handling difficulties during loading and recovery in each cycle, (ii) increased pressure drop and greater tendency for particle agglomeration and channelling in the reactor, (iii) higher susceptibility to mechanical loss and entrainment during repeated reaction cycles, (iv) reduced reproducibility of the experimental results under the operating conditions used in this work. It may provide a higher reaction rate due to increased external surface area and improved accessibility of the active Pt sites, but it has several observed practical limitations. If the particle size is further increased, the reaction is no longer purely kinetically controlled. Still, it involves a diffusion contribution, particularly intra-particle mass transfer resistance, which reduces the effective utilization of catalytic sites. In contrast, the 68 µm catalyst exhibited stable performance, good recyclability, and consistent hydrazine destruction efficiency over multiple cycles. Therefore, this particle size was considered more suitable for the objectives and operating conditions of the current study.

Table 5: Influence of Catalyst Amount in Comparison on the Apparent First-Order Rate Constants (K) of Decomposition of Hydrazine in Nitric Acid on Pt/Sio_2 Catalyst

	Rate constant, min^{-1}		
Catalyst amount, g	20 micron	38 micron	68 micron
0	0.032	0.025	0.016
4	0.052	0.037	0.033
6	0.071	0.067	0.044
8	0.103	0.089	0.073
10	0.124	0.115	0.098

3.3. Effect of temperature

As the next step in the optimization process, the influence of temperature on the decomposition of hydrazine in a nitric acid medium over the Pt/SiO_2 catalyst was studied. In the literature, it is reported that, for many catalysts, increasing the reaction temperature increases

activity [9-15, 17-19, 22-25, 31-33]. To confirm this trend, the experiment was performed by varying the temperature from 313 to 343 K, with the experimental conditions optimized in the previous section, as shown in Table 2. The linearity of $\ln(C/C_o)$ vs. time plots displayed in Fig. 7 exhibited good correlation (R^2 = 0.972 to 0.878), confirming that the decomposition of hydrazine follows pseudo-first-order kinetics except at higher nitric acid concentrations, where deviations were observed due to competitive adsorption effects. This suggested that the rate of hydrazine decomposition depends directly on its bulk concentration, consistent with a charge-transfer-controlled reaction under the applied conditions. The apparent rate constant (k) increased with temperature, indicating that higher temperature enhanced electron transfer or improved mass transport of hydrazine to the surface reaction sites on Pt. However, a slight deviation from strict proportionality between k and temperature (particularly at 343 K) may be attributed to mass-transfer limitation and gas bubble coverage on the surface, which reduced the effective active area. These results confirmed that, within the studied temperature range, hydrazine decomposition follows pseudo-first-order kinetics with respect to hydrazine concentration and temperature increases; the decomposition rate increases as predicted by the Arrhenius equation. The activation energy was calculated from the slope of ln(k) vs. 1/T (Fig. 8) and was found to be 47.88kJ/mol, over the temperature range 313-343K. The temperature dependence of the rate constant is as follows:

$$k = Ae^{-E_a/RT} \qquad \ln k = \ln A - \frac{E_a}{RT}$$

Where k is the rate constant, A is the pre-exponential factor, T is the absolute temperature, E_a is the activation energy, and R is the gas constant (8.314 J mol^{-1} K^{-1}). The decomposition rate increased exponentially with temperature due to the higher kinetic energy of reactant molecules and improved diffusion of hydrazine species to the catalyst surface, and Arrhenius analysis yielded apparent activation energies significantly lower than those observed in non-catalytic systems, confirming the catalytic role of Pt. The moderate activation energy indicated that the reaction is catalyst surface-controlled, with minimal internal diffusion and strong interaction between hydrazine and the Pt active sites. At higher nitric acid concentrations, a slight increase in E_a was observed, which may be attributed to competitive adsorption between hydrazine and nitrate ions, reducing the availability of Pt active sites. At higher temperatures, decomposition occurred even more rapidly, but sample collection was not feasible, and analysis was not reproducible. Hence, the temperature was set to 333 K for hydrazine decomposition studies.

The influence of particle size on the reaction kinetics was examined using a Pt/SiO_2 catalyst with varying particle sizes. The observed rate constants summarized in Table 6 decreased with increasing particle sizes. This may increase the external surface area for smaller particles, improve the accessibility of Pt active sites, and reduce mass transfer resistance. For a smaller particle size, the reaction rate is predominantly controlled by intrinsic kinetics. However, as particle size increases, external diffusion resistance begins to influence the overall rate, leading to lower observed rate constants.

Table 6: Influence of Temperature in Comparison on the Apparent First-Order Rate Constants (K) of Decomposition of Hydrazine in Nitric Acid on Pt/Sio_2 Catalyst

	Rate constant, min^{-1}		
Temp, K	20 micron	38 micron	68 micron
313	0.4328	0.2634	0.1193
323	0.6032	0.3523	0.1764
333	0.8354	0.4105	0.2575
343	1.7498	0.9885	0.5147

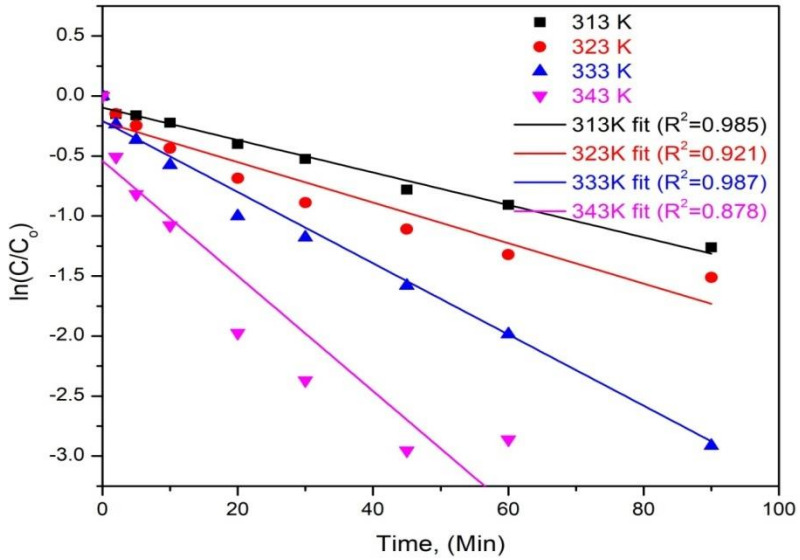

Fig.7: Influence of Temperature on the First-Order Kinetic Plots for the Decomposition of Hydrazine Over Pt/Sio_2. $[N_2H_4]$ = 0.5 M, $[HNO_3]$ = 1.5 M, RPM = 500, Catalyst Amount = 8 G, Varying Temperature from 313 to 343 K.

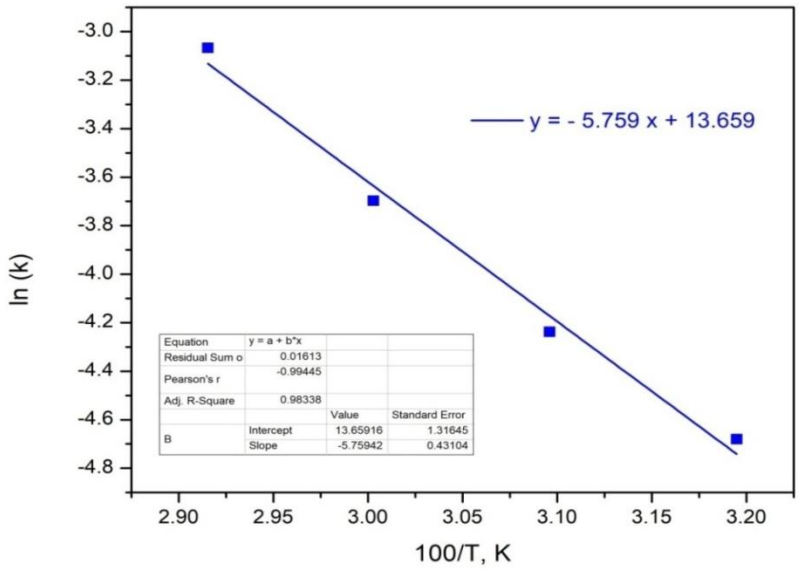

Fig. 8: Arrhenius Plot of Initial Rate on Hydrazine Decomposition.

3.4. Effect of nitric acid on reaction kinetics

The influence of nitric acid on the decomposition of hydrazine in nitric acid solution was studied in the presence of the solid catalyst Pt/SiO_2. Here, 100 mL of a 0.5 M hydrazine stock solution in 2.5 M nitric acid was taken in a glass reactor. Experiments were carried out with optimized parameters: reaction temperature of 333 K, catalyst amount of 8 g, and two-phase stirring rate of 500 rpm. Samples were collected at predetermined intervals and analyzed. The kinetic data were initially analyzed using a pseudo-first-order method by plotting $\ln(C/C_o)$ vs. time at different nitric acid concentrations under the experimental conditions, as shown in Fig. 9. Unlike the trends observed for other operational parameters such as catalyst loading, mixing speed, and temperature, the ln(C/Co) plots for nitric acid concentration exhibited significant deviation from linearity. The coefficient of determination (R^2) ranged from 0.7 to 0.9, indicating poor conformity to first-order kinetics. This may be due to competitive adsorption of nitric acid on the Pt surface, which blocks hydrazine adsorption. It plays a dual role in the reaction system: it participates in the reaction medium and simultaneously acts as an inhibitor by competing with hydrazine for active sites on the Pt surface, reducing the availability of active sites for hydrazine decomposition. To account for the observed non-linearity, the kinetic data were analyzed using the Langmuir-Hinshelwood model [34-37], which incorporates adsorption of both hydrazine and nitric acid on the catalyst surface. The rate expression is given by:

$$r_s = k_s K_A K_B \frac{C_A C_B}{(1 + K_A C_A + K_B C_B)^2}$$

Where A and B are reactants, C_A and C_B are the concentrations of hydrazine and nitric acid (g moles/L), $k_s$is the rate constant, and K_A and K_B are the adsorption rate constants of A and B. The rate parameters of the model equation were estimated from experimental data and are shown in Fig. 10. This provides a more accurate description of the reaction kinetics under these conditions. Since plant conditions for nuclear fuel reprocessing using hydrazine are restricted to 1.5 M nitric acid, the studies reported here are conducted in this medium. The quantitative kinetic fitting parameters obtained from the Langmuir–Hinshelwood (L–H) kinetic analysis have been summarized in Table 7. The proposed elementary steps of the Langmuir-Hinshelwood model are described below.

Table 7: Kinetic Fitting Parameters Obtained from the Langmuir–Hinshelwood Model

[HNO_3], M	k_{app} (min^{-1})	R^2	Std. Error
1.5	0.02470	0.9120	0.00313
2.5	0.02173	0.7332	0.00535
3.0	0.02260	0.7034	0.00599

The catalytic decomposition of hydrazine in nitric acid over Pt/SiO_2 proceeds via a heterogeneous pathway involving adsorption of reactants on catalyst active sites. Based on the established Langmuir–Hinshelwood (L–H) mechanism, where both reactants adsorb onto a catalytic surface and react there. The proposed elementary steps are:
Adsorption of hydrazine (A) & nitric acid (B) on the catalyst surface:

$$N_2H_4 + S \rightarrow N_2H_4 \cdot S \quad (1)$$

$$HNO_3 + S \rightarrow HNO_3 \cdot S \quad (2)$$

Surface reaction (rate-determining step):

$$N_2H_4 \cdot S + HNO_3 \cdot S \rightarrow \text{Product} \quad (3)$$

Where S = vacant catalytic site,

At adsorption equilibrium $K_A = \frac{\theta_A}{C_A\theta_S}$; $K_B = \frac{\theta_B}{C_B\theta_S}$ (4)

$\theta_A = K_AC_A\theta_S$ and $\theta_B = K_BC_B\theta_S$ (5)

Total active sites: $\theta_S + \theta_A + \theta_B = 1$ (6)

Where θ_A surface coverage of hydrazine and θ_B surface coverage of nitric acid

$\theta_S + K_AC_A\theta_S + K_BC_B\theta_S = 1; \theta_S(1 + K_AC_A + K_BC_B) = 1$ (7)

$\theta_S = \frac{1}{(1+K_AC_A+K_BC_B)}$ (8)

The fractional surface Expressions:

$\theta_A = \frac{K_AC_A}{1+K_AC_A+K_BC_B}$ and $\theta_B = \frac{K_BC_B}{1+K_AC_A+K_BC_B}$ (9)

Where K_A, K_B= adsorption equilibrium constants and C_A, C_B = concentrations of hydrazine and nitric acid. The rate is proportional to the surface reaction: $r = k\theta_A\theta_B$; substituting the values

$r = k\frac{K_AC_A}{1+K_AC_A+K_BC_B} \cdot \frac{K_BC_B}{1+K_AC_A+K_BC_B} = k\frac{K_AC_AK_BC_B}{(1+K_AC_A+K_BC_B)^2}$ (10)

Finally, the rate law is $r = k\frac{K_AK_BC_{N_2H_4}C_{HNO_3}}{(1+K_AC_{N_2H_4}+K_BC_{HNO_3})^2}$ (11)

Under the typical experimental conditions, hydrazine concentration is constant (0.55 M) and nitric acid concentration is varied.So, simplify the equation.

$r = \frac{k'C_{HNO_3}}{(1+K_BC_{HNO_3})^2}$ (12)

where $k' = k K_AC_A$. The L-H model explains the non-linear dependence of rate on nitric acid concentration, (i) at low concentrations, rate is second order due to both hydrazine and nitric acid involved in the reaction, (ii) at very high concentration, rate is zero order due to surface become saturated, (iii) if one reactant concentration is in excess, then rate may appear pseudo first order reaction.

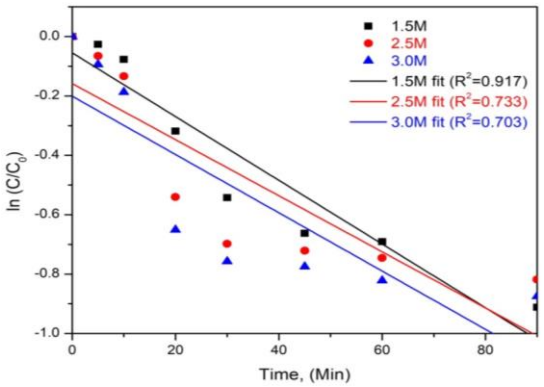

Fig. 9: Influence of Nitric Acid on the First-Order Kinetic Plots for the Decomposition of Hydrazine Over Pt/Sio_2. $[N_2H_4]$ = 0.5 M, RPM = 500, Catalyst Amount = 8 G, Temp = 333 K, Varying $[HNO_3]$ from 1.5 to 3M.

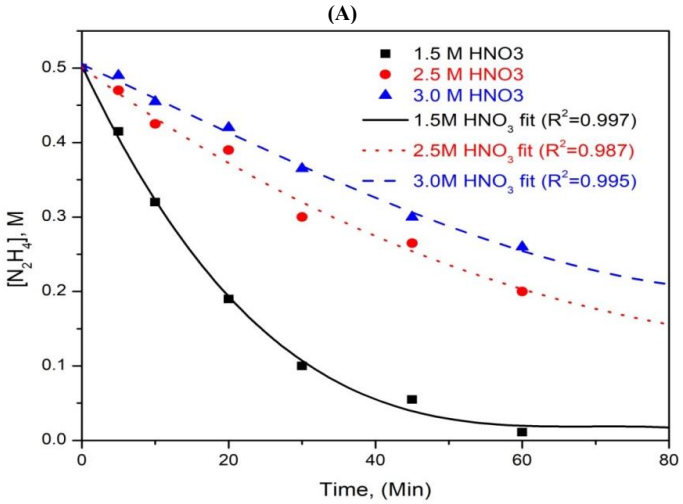

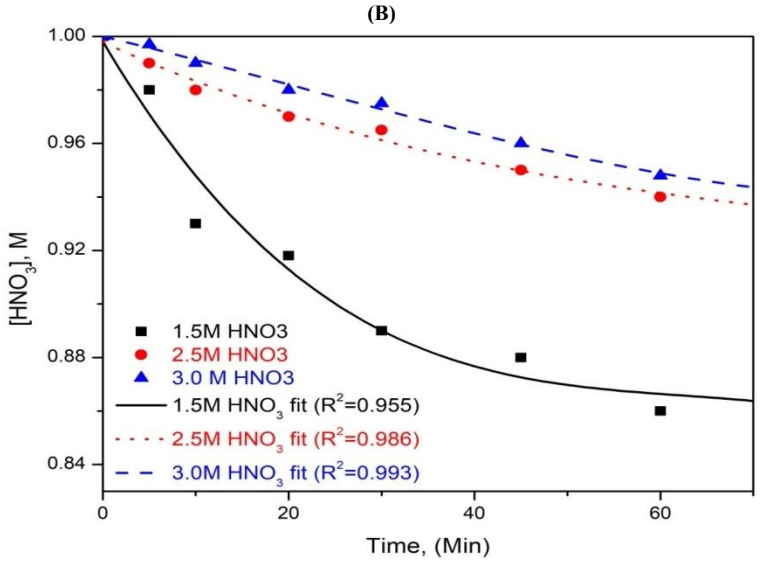

Fig. 10: Reaction Kinetics of Decomposition of Hydrazine Using Langmuir-Hinshelwood Model in Terms of(A) Hydrazine and (B) Nitric Acid Concentrations.

3.5. Reusability studies

To assess the stability of the catalytic material through the consecutive batch decomposition of hydrazine under experimental conditions (0.5 M hydrazine, 1 M nitric acid, mixing speed 500 rpm, and temperature 333K) with a catalyst amount of 8 g. In the reusability studies, the catalyst was separated from the reaction mixture through simple filtration and directly reused in subsequent experiments without requiring additional purification steps. The reusability profile of the Pt/SiO_2 catalyst for hydrazine decomposition in nitric acid medium shows variation of hydrazine decomposition (%) as a function of reuse cycle under identical conditions and is shown in Fig. 11.

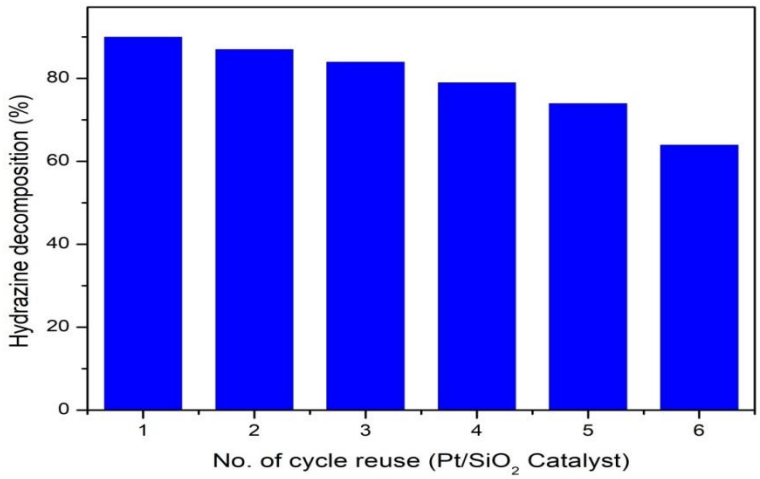

Fig. 11: Reusability of Pt/Sio_2Catalyst for the Decomposition of Hydrazine.

The results demonstrate that the Pt/SiO_2 catalyst retains significant catalyst activity over 5 cycles, demonstrating its robustness in a highly acidic medium, and completely decomposes hydrazine nitrate during 5 reuse cycles. As the number of reusability cycles increased, reaction time decreased gradually, and catalyst activity increased, indicating a reactivation stage. Subsequently, from the 6th time onward, hydrazine decomposition fluctuated, with discrete distribution patterns and an overall decline in catalyst activity. The apparent rate constant for hydrazine decomposition was calculated for each reuse cycle, assuming a pseudo-first-order reaction with respect to hydrazine concentration. It revealed that the marginal decrease in the apparent rate constant with successive cycles suggests that the catalytic mechanism (such as the Langmuir-Hinshelwood mechanism involving adsorption of hydrazine on the Pt surface) remains unchanged, even though the number of active sites may decrease slightly.

4. Conclusion

The catalytic decomposition of hydrazine nitrate in nitric acid medium has been systematically investigated under conditions relevant to PUREX process streams. The results demonstrate that the Pt/SiO_2 catalyst effectively promotes hydrazine decomposition in nitric acid medium and determine the reaction kinetics and temperature dependence. The reaction follows first-order kinetics with respect to hydrazine nitrate concentration. The Arrhenius analysis yielded an activation energy of approximately 47.88 kJ mol^{-1}, indicating that the reaction proceeds through a surface-controlled catalytic pathway. The decomposition rate increases with increasing catalyst loading and temperature. Nitric acid concentration significantly influences the reaction by affecting hydrazine protonation and catalyst surface interactions. Increasing the rotating speed enhances mass transfer but has little effect once the reaction becomes kinetically controlled. The findings suggest that Pt/SiO_2 catalysts may provide an efficient approach for treating hydrazine-containing nitric acid streams in nuclear fuel reprocessing facilities that employ the PUREX process.

Acknowledgement

The authors would greatly appreciate the timely support and guidance of the present and past associate directors and directors of the Reprocessing Group. The authors are also grateful to the technical support rendered by Dr. N. Desigan, MACS, and Shri P. Rajeev, RpMDS, Reprocessing Group, IGCAR, Kalpakkam.

Declaration of Generative AI Use

During the preparation of this work, the author(s) used ChatGPT (OpenAI, version GPT- 4o) to improve the readability and language clarity during preparation of the manuscript. After using this tool, the author(s) reviewed and edited the content as needed and take full responsibility for the content of the published article.

Declaration of Conflict of Interest

The authors declare that they have no known competing financial interests or personal relationships that could have appeared to influence the work reported in this paper.

References

[1] Natarajan, R. (2017). Reprocessing of spent nuclear fuel in India: Present challenges and future programme, Prog. Nucl. Energy, 101, 118-132. https://doi.org/10.1016/j.pnucene.2017.03.001.

[2] Kodandaraman, J., Anandarao, B.M., Shekhar Kumar, Rajan, K., Pandey, N.K., Ravisankar, A. (2017). Concurrent trends in Indian fast reactor fuel reprocessing, Report No. IAEA-CN-245,

[3] Pandey, N.K., Desigan, N., Ramanujam, A. (2016). PUREX and Thorex processes (Aqueous Reprocessing), Ref. Module in Mat. Sci. and Mat. Engg, Elsevier, 1-15. https://doi.org/10.1016/B978-0-12-803581-8.02094-4.

[4] He, H., Ye, G., Tang, H., Zheng, W., Li, G., Lin, R. (2014). An advanced PUREX process based on salt-free reductants, Radiochimica Acta, 102, 127-133. https://doi.org/10.1515/ract-2014-2120.

[5] Sun, X., Ceo, Z., Zuo, C., Chen, Q., Li, T., Zheng, W. (2026). Impact of various reductants on Pu (III) stability in the organic phase and its distribution ratio in a biphasic system, New. J. Chem, 50, 34-46. https://doi.org/10.1039/D5NJ03511B.

[6] Oriov, S.N., Zmitrodan, A.A., Mysik, S.G. (2018). Effect of hydrazine on redistribution of corrosion product deposits in the primary circuit of a shutdown reactor in propulsion-type nuclear power reactor, Thermal Engineering, 65,217-221.https://doi.org/10.1134/S0040601518040067.

[7] Wattal, P.K. (2017). Back end of Indian nuclear fuel cycle - a road to sustainability, Prog. Nucl. Energy, 101, 133-145.https://doi.org/10.1016/j.pnucene.2017.03.004.

[8] Brahmananda Rao, C.V.S., Achutan, P.V., Sivaraman, N. (2025). Nuclear fuel reprocessing, in Nuclear fuel cycle, edited by Tomar, B.S., Rao, P.R.V., Roy, S.B., Panakkal, J.P., Raj, K., Nandakumar, A.N. Springer Nature, p 213-253.https://doi.org/10.1007/978-981-99-0949-0_7.

[9] Kalistratova, V., Obedkov, A., Belova, E. (2017).Kinetic model of thermal decomposition of nitric acid solutions of hydrazine nitrate, Thermochimica Acta, 742, 179876.https://doi.org/10.1016/j.tca.2024.179876.

[10] Izato, Y., Shiota, K., Miyake, A. (2022). Detailed kinetic model for the thermal decomposition of hydrazine nitrate in nitric acid solution, J.Phys. Chem. A, 126, 2998-3005.https://doi.org/10.1021/acs.jpca.2c00629.

[11] Ananiev, A.V., Tananaev, I.G., Shilov, V.P. (2005). Heterogeneous catalytic redox reactions in the chemistry and technology of the nuclear fuel cycle. Russian Chemical Reviews, 74 (11), 1039-1059.https://doi.org/10.1070/RC2005v074n11ABEH001186.

[12] Zhang, Z., Li, B., Chen, Q., Chen, X., Yan, T., Zheng, W., Zuo, C. (2022). Catalytic decomposition of hydroxylamine nitrate and hydrazine nitrate using Ru/ZSM-5 catalyst under mild reaction conditions, RSC Advances, 12, 4469-4474. https://doi.org/10.1039/D1RA07724D.

[13] Li, B., He, T., Zuo, C., Cao, Z., Yan, T., Zheng, W. (2023).The reaction kinetics and mechanism of catalytic decomposition of hydrazine nitrate on Ru/C catalyst in nitric acid solutions, New J. Chemistry,47, 7583-7587. https://doi.org/10.1039/D3NJ00193H.

[14] Yu, D., Li, B., Cao, Z., Chen, Q., Zuo, C., He, T., Yan, T., Zheng, W. (2024). Catalytic decomposition of hydrazine nitrate and hydroxylamine nitrate in radioactive nitric acid waste liquid using Ru/AC catalyst. New J. Chemistry, 48, 8660-8666. https://doi.org/10.1039/D4NJ00916A.

[15] Li, B., Hao, S., Zhang, Q., Xia, L., He, H. (2024). Free radical generation from hydrazine decomposition catalyzed by Pt/SiO_2 in different acid–base systems. J. Nucl. Radiochem, 46 (1), 54-59.

[16] Yu, X., Zhang, L., Chen, H., Li, Y. (2025). Synergistic effect boosting the decomposition of hydrazine nitrate on bimetallic Pt–Ru/SiO_2 catalysts. Chem. Eng. J., 510,161598. https://doi.org/10.1016/j.cej.2025.161598.

[17] Wang, X., Liu, Y., Chen, Z., Zhang, H. (2005). Catalytic decomposition of hydrazine nitrate and hydroxylamine nitrate using supported metal catalysts.RSC Adv., 12, 14263-14272.

[18] Zhang, L., Sun, J., Liu, Y., Li, Y. (2025). Adsorption and decomposition kinetics of hydrazine nitrate on transition metal surfaces. Langmuir, 41, 28866–28882.https://doi.org/10.1021/acs.langmuir.5c04496.

[19] Z. Cao, Z., D. Yu, D., He, T., Li, T., Zuo, C., Li, B., Lv, H., Yan, T., Zheng, W. (2025). The Effect of Activated Carbon Support on Ru/AC Catalysts Used for the Catalytic Decomposition of Hydroxylamine Nitrate and Hydrazine Nitrate, Processes, 13, 641. https://doi.org/10.3390/pr13030641.

[20] Singh, S.K., Xu, Q. (2010). Bimetallic Ni–Pt nano catalysts for selective decomposition of hydrazine to hydrogen in aqueous solution, Inorg. Chem., 49, 6148–6152. https://doi.org/10.1021/ic1007654.

[21] Zhou, L., Luo, X., Xu, L., Wan, C., Ye, M. (2020). Pt-Ni nanoalloys for H_2 generation from hydrous hydrazine, Catalysts, 10(8), 30. https://doi.org/10.3390/catal10080930.

[22] Tyumentsev, M.S., Ananiev, A.V., Lapitskaya, T.S. (2013). Catalytic decomposition of hydrazine on ruthenium catalysts in nitric acid solutions, Radiochemistry, 55, 279-286. https://doi.org/10.1134/S1066362213030065.

[23] Abdounnabi, H.M., Ananiev, A.V. (2003). Platinum catalyzed hydrazine decomposition in acidic media, Appl. Catal. A: Gen., 242, 1–10. https://doi.org/10.1016/S0926-860X(02)00368-X.

[24] Ananiev, A.V., Shilov, S.P. (2004). Heterogeneous catalytic decomposition of hydrazine in nitric acid solutions. Radiochemistry, 46, 377-384. https://doi.org/10.1023/B:RACH.0000039116.09002.c8.

[25] Matyshak, V.K., Silchenkova, O.N. (2022). Catalytic decomposition of hydrazine and hydrazine derivates to produce hydrogen-containing gas mixtures: A Review, Kinetics and catalysis, 63 (4), 339-350. https://doi.org/10.1134/S0023158422040073.

[26] Khan, W.U., Hantoko, D., Osman, A.I., Nasr, M., Rashwan, A.K., Gambo, Y., Shoaibi, A.A., Chandrasekar, S. (2023). Recent progress for hydrogen production from ammonia and hydrous hydrazine decomposition: A Review on heterogeneous catalysts, Catal. Today, 423, 114022. https://doi.org/10.1016/j.cattod.2023.01.029.

[27] Reddy, R.K., Pandey, N.K., Mondal, S., Sivaraman, N. (2020). Catalytic reduction of U(VI) with hydrazine using Pt/SiO2 catalyst in nitric acid medium – kinetics and equilibrium, J. Radioanal. Nucl. Chem. 325, 425-434. https://doi.org/10.1007/s10967-020-07265-8.

[28] Ganesh, S., Khan, F., Ahmed, M.K., Pandey, S.K. (2011). Potentiometric determination of free acidity in presence of hydrolysable ions and a sequential determination of hydrazine, Talanta, 85 (2), 958-963. https://doi.org/10.1016/j.talanta.2011.05.001.

[29] Ganesh, S., Khan, F., Ahmed, M.K., Pandey, S.K. (2010). Sequential determination of uranium (IV), free acidity and hydrazine in a single aliquot, J. Radioanal. Nucl. Chem. 286, 33-37. https://doi.org/10.1007/s10967-010-0663-9.

[30] Ganesh, S., Khan, F., Ahmed, M.K., Velavendan, P., Pandey, N.K., Mudali, U.K. (2012). Spectrophotometric determination of hydrazine with para-dimethylaminobenzaldehyde in aqueous streams of PUREX process. Int. J. Nucl. Sci. Engg., 2, 1-4.

[31] Pandey, N.K., Reddy, R.K., Mishra, S.B., Murali, R., Joshi, J.B. (2018). Study on the kinetics of catalytic hydrogenation of U(IV) in the nitric acid solution using a bubble reactor, Ind. Eng. Chem.Res.,57 (10), 3482-3488. https://doi.org/10.1021/acs.iecr.7b04293.

[32] Reddy, V., Dai, H., Zhong, Y., Wang, B. (2017). Hydrogen generation from decomposition of hydrous hydrazine over Ni-Ir/CeO_2 catalyst, Prog. Nat. Sci. Mat. Int., 27, 121-125. https://doi.org/10.1016/j.pnsc.2016.12.012.

[33] Kitson, B.A., Oliaee, S.N. (2016). Selective catalytic decomposition of hydrazine, Honors Research Projects, Willims Honors College, 286, https://ideaexchange.uakron.edu/ honors_research_projects/286.

[34] Baek, B., Fickel, D., Kimmenade, E., Barton, K. (2025). Langmuir-Hinshelwood kinetic model for butane hydrogeneolysis on Ir-Pt/Al_2O_3/ZSM-5, Ind. Eng. Chem. Res., 64 (19), 9591-9599. https://doi.org/10.1021/acs.iecr.5c00445.

[35] Kiani, D., Wachs, I.E. (2007). Reactor the conundrum of pair sites in Langmuir-Hinshelwood reaction kinetics in heterogeneous catalyst, ACS Catal., 14, 10260-10270. https://doi.org/10.1021/acscatal.4c02813.

[36] Alvarex-Ramirex, J., Ochoa-Tapia, J.A., Viveros, T. (2026). Langmuir-Hinshelwood kinetics: a singular value decomposition perspective on the quasi-steady state assumption, Reac. Kinet. Mech. Cat., 139, 71-97. https://doi.org/10.1007/s11144-025-02953-6.

[37] Adamou, P., Bellomi, S., Harkou, E., Chen, X., Delgado, J.J., Deimitratos, N., Manos, G., Villa, A., Constantinou, A. (2024). Hydrous hydrazine decomposition over Rh/Al_2O_3 catalyst: Experimental and CFD studies, Chem. Engg. J., 493, 152715.https://doi.org/10.1016/j.cej.2024.152715.